S^2 Measurements Showing Suppression of Higher Order Modes in Confined Rare Earth Doped Large Core Fibers

Stefan Gausmann, Jose E. Antonio-Lopez, James Anderson, Steffen Wittek, Sanjabi Eznaveh Eznaveh, Hee-Jun Jang, Md Selim Habib, Justin Cook, Martin C. Richardson, Rodrigo Amezcua Correa, and Axel Schülzgen, *Fellow, IEEE*

***Abstract*—We present a detailed investigation on higher order mode suppression due to differential gain in large mode area step index fiber amplifiers with confined Yb doping using spatially and spectrally resolved imaging (S^2). A novel active fiber with Yb doping confined to the central 30% of the core area is fabricated and its performance is directly compared to a fiber with a conventional homogeneously doped core with almost identical parameters. At high pump rates, S^2 and beam pointing stability measurements clearly demonstrate fundamental mode operation of the confined doping few mode fiber, even under imperfect launching conditions and environmental perturbations. In addition, we discuss the mode content as a function of gain in co-pumped fiber amplifiers with and without confined rare earth core doping using a power propagation model for fibers with similar parameters to those used in our experiments. Our simulation results as well as amplification experiments indicate the great potential of the confined doping concept for single mode high power operation.**

***Index Terms*—Doped fiber amplifiers, fiber lasers, optical fibers.**

I. Introduction

LARGE mode area (LMA) step index fibers with large core diameters and small numerical apertures (NAs) are essential for the development of kW class fiber lasers with nearly diffraction limited beam quality [1]. The LMA concept mitigates power limiting nonlinear effects such as stimulated Brillouin scattering (SBS) and stimulated Raman scattering (SRS) [2]. Mode area scaling while preserving single mode guidance is challenging in step index waveguides as the core NA cannot be chosen to be arbitrarily small and the number of supported modes increases intrinsically as the core becomes larger. Therefore, it is common practice to use LMA few mode fibers for both high power fiber laser oscillators and amplifiers [3]–[6]. The majority of strategies, that have been developed over the years to suppress the unwanted higher-order-modes (HOMs) in LMA fibers, exploit differential propagation losses between the fundamental mode and HOMs [7]–[12]. An alternative approach relies on tailoring the transversal rare earth core doping profile in LMA fibers to provide preferential gain to the fundamental mode [13]. While loss induced HOM suppression in LMA fibers has been investigated extensively in the past [14]–[17], experimental results on HOM suppression due to differential gain in LMA step index fibers are rare [18]–[20]. In particular, the effectiveness of modal gain filtering by moving away from a homogeneously doped cores towards a so-called confined doping approach, where the rare earth doping is limited to the central part of the fiber core, has only been investigated qualitatively by measuring the beam quality factor M^2 and the beam pointing stability [21]–[25].

In this work, we discuss the concept of gain induced high order mode suppression numerically on the example of few mode fibers ($V = 3.5$) using a power propagation model, which includes spatial gain depletion in the core region, for co-pumped fiber amplifiers. We further present two novel low NA LMA fibers that have been fabricated in-house. The ytterbium doping of the first fiber (Fiber 1) is distributed homogenously across the entire core region while the Ytterbium doing of the second fiber, Fiber 2, is only confined to the central region of the core, to provide preferential gain to the fundamental mode. Finally, we quantify for the first time the HOM content of the signal beam after amplification in a LMA fiber with confined core doping, Fiber 2, as a function of absorbed pump power using spatially and spectrally resolved imaging (S^2) [26]. As a direct reference, we perform the same analysis using the very similar LMA step index fiber with homogenous Ytterbium doping across the entire core, Fiber 1. In addition, we present a pointing stability analysis of beams exiting the confined doping fiber amplifier in the

Manuscript received September 24, 2019; revised December 4, 2019; accepted January 13, 2020. Date of publication January 23, 2020; date of current version April 1, 2020. This work was supported in part by the U.S. Department of Commerce under Grant BS123456, in part by United States Army Research Office under Grant W911NF-12-1-0450, Grant W911NF-17-1-0501, and Grant W911NF-19-1-0426, and in part by the United States Air Force Office of Scientific Research under Grant FA9550-15-10041. *(Corresponding author: Stefan Gausmann.)*

S. Gausmann, J. E. Antonio-Lopez, J. Anderson, S. Wittek, S. E. Eznaveh, H.-J. Jang, J. Cook, M. C. Richardson, R. A. Correa, and A. Schülzgen are with the College of Optics and Photonics at the University of Central Florida, Orlando, FL 32816 USA (e-mail: stefan.gausmann@knights.ucf.edu; jealopez@creol.ucf.edu; jkanderson@knights.ucf.edu; swittek@knights.ucf.edu; zahoora@knights.ucf.edu; heejunjang@knights.ucf.edu; jcook5610@knights.ucf.edu; mcr@creol.ucf.edu; r.amezcua@creol.ucf.edu; axel@creol.ucf.edu).

M. S. Habib is with the College of Optics and Photonics at the University of Central Florida, Orlando, FL 32816 USA, and also with the Florida Polytechnic University, Department of Electrical and Computer Engineering, Lakeland, Fl-3380 USA (e-mail: mhabib@floridapoly.edu).

This letter has supplementary downloadable material available at https://ieeexplore.ieee.org, provided by the authors.

Color versions of one or more of the figures in this article are available online at https://ieeexplore.ieee.org.

Digital Object Identifier 10.1109/JLT.2020.2969012

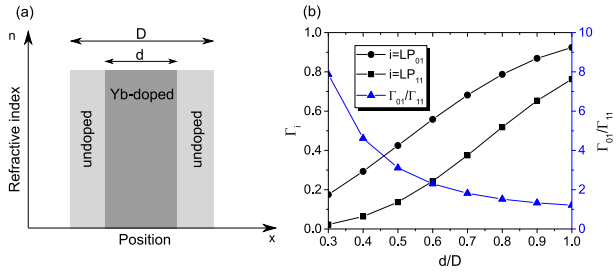

Fig. 1. (a) Illustration of the refractive index profile of a confined doping fiber with core diameter D and Ytterbium doping diameter d. (b) Left axis (black symbols and lines): Gain overlap factors of LP_{01} and LP_{11} mode as a function of d/D. Right axis (blue triangles and line): Ratio of the small signal gains of LP_{01} and LP_{11} modes as a function of d/D.

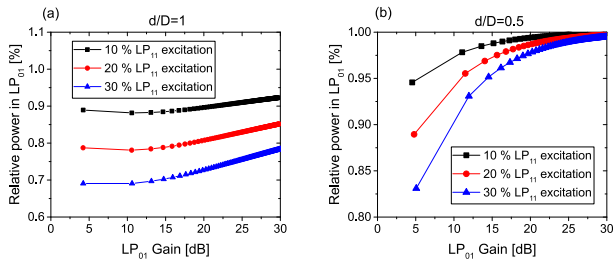

Fig. 2. (a) Relative fundamental mode power after amplification as function of fundamental mode gain for fiber with homogeneous core doping d/D = 1. (b) Relative fundamental mode power after amplification as function of fundamental mode gain for fiber with confined core doping d/D = 0.5.

presence of environmental perturbations. Both S^2 measurements as well as our pointing stability analysis, clearly demonstrate HOM suppression due to differential gain in the confined doping amplifier at high pump rates. These findings, in combination with recent high power experiments [27], make our confined doping fiber highly promising for high power fiber laser systems with robust single mode performance.

II. Confined Doping Concept

Tailoring the transverse Ytterbium doping profile in LMA few mode fiber cores can result in discrimination against HOMs on account of different gain when the overlap of the fundamental mode is significantly larger than the overlap of HOMs with the Ytterbium doped region of the core. Confining the Ytterbium doping to the central core region is in particular effective if the normalized frequency parameter V of the waveguide is below 3.8, as the only guided HOMs ($LP_{11,a}$ and $LP_{11,b}$) have intensity minima in the center of the core. A schematic of the refractive index profile of a step index waveguide with a core diameter D and a confined Ytterbium doped region with a diameter $d < D$ is shown in Fig. 1(a). To illustrate the gain advantage of the fundamental mode over HOMs in such a confined doping fiber, we calculated gain overlap factors Γ_{01} and Γ_{11} of the fundamental LP_{01} mode and the higher order LP_{11} modes for fibers with a core with diameter $D = 23$ μm and core NA of 0.05 at a wavelength of 1060 nm for a variety of d/D ratios. The small signal gain ratio $g_{01}/g_{11} = \Gamma_{01}/\Gamma_{11}$ of the LP_{01} and LP_{11} modes is with 1.3 rather small for a homogenously doped fiber (d/D = 1) compared to a small signal gain ratio of almost 8 for a confined doping fiber with d/D = 0.3 (Fig. 1(b)).

Imperfect launching conditions or mode scattering along the fiber, can result in unwanted HOM content in LMA fiber amplifiers. To illustrate the impact of differential gain on the mode purity after amplification and to understand the physics of gain filtering in more detail, full numerical simulations of LMA fiber amplifiers have been performed similar to [28]. Our simulations assume 976 nm co-pumping, a circular pump cladding with 400 μm diameter, an Ytterbium doping concentration of 4.5×10^{25} ions/m^3 and fiber lengths that guarantee 99% absorption of the pump power. We assume a signal wavelength of 1060 nm and an initial signal power of 10 W, which is well above the saturation power. Imperfect seed launching conditions are simulated by splitting the power that is not launched into fundamental mode equally between the LP_{11a} and LP_{11b} modes at the beginning of the amplifier. Fig. 2 illustrates the relative power in the LP_{01} mode after amplification as a function of LP_{01} gain for 10%, 20% and 30% of initial total LP_{11} content and for two different Ytterbium doping profiles. For a fiber amplifier with homogenous core doping (d/D = 1), and for small amounts of LP_{11} content (<30%) as well as fundamental mode gains <10 dB, the HOM content increases, as the gain of the fundamental mode in the center of the core saturates before the gain of the LP_{11} at the core edge does (see Fig. 2(a)). For fundamental mode gains above 15 dB, both the fundamental mode gain as well as the HOM gain are saturated and the larger overlap of the fundamental mode with the doped core results in a slight increase in output mode purity. Gain saturation effects of the fundamental mode play a less import role for the second fiber with confined core doping (d/D = 0.5) as the overlap of the LP_{11} modes with the gain is much smaller than in the first case. Our model predicts that about 10 dB fundamental mode gain is sufficient to suppress the LP_{11} content efficiently in a confined doping fiber with d/D = 0.5 and more than 97% fundamental mode content can be achieved for typical amplifier gains of 20 dB (see Fig. 2(b)).

III. Fiber Fabrication and Characterization

Two fibers with very similar core sizes, core NAs, and Yb doping concentrations have been fabricated in-house allowing for a direct performance comparison. The first fiber, referred to as "Fiber 1", is a low NA step index fiber with homogenous Yb doping across the entire core region. The Yb doping of the second fiber, referred to as "Fiber 2", has been confined to the central region of the core by surrounding a Yb-doped silica rod in the center of the core with a Ge-doped silica ring. The Ge doping concentration was chosen to closely match the refractive index of the Yb-doped material. Scanning electron microscope (SEM) images and 2D refractive index measurements for Fiber 1 and Fiber 2 are presented in Figs. 3(a) and 3(b), and Figs. 3(c) and 3(d), respectively. In contrast to the flat refractive index profile of Fiber 1, our confined doping fiber shows a small index step of 2×10^{-4} across the core region – due to the use of Yb-doped and Ge-doped material during the core manufacturing process. In contrast to previously reported LMA fibers with confined Yb doping [21]–[25], our fabrication method allows for more

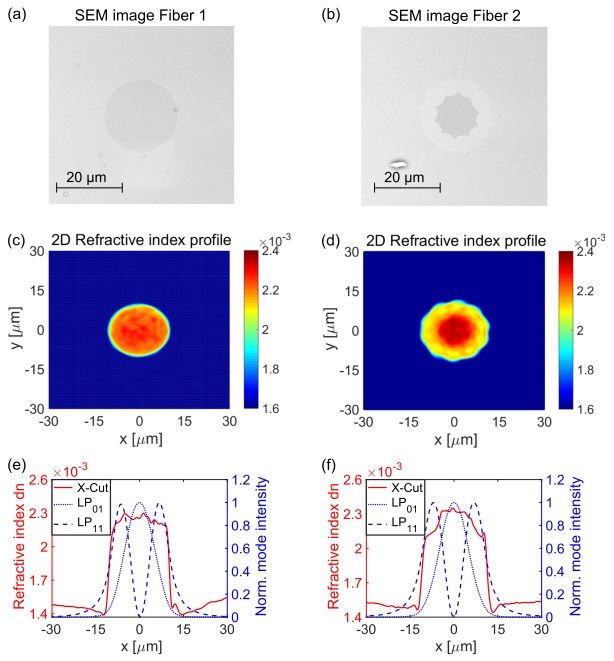

Fig. 3. (a), (b) SEM images (taken with Phantom ProX by Thermo Fisher Scientific) of the core regions of Fiber 1 and Fiber 2, respectively. (c), (d) 2D Refractive index profiles (measured with IFA-100 by Interfiber Analysis) of Fiber 1 and Fiber 2, respectively. (e), (f) 1D Refractive index profiles (red) and simulated mode profiles (blue) based on the measured refractive index data for Fiber 1 and Fiber 2, respectively (simulations performed with FIMMWAVE by Photon Design).

TABLE I
FIBER PARAMETERS

	Fiber 1	Fiber 2
Total core diameter	22 µm	23 µm
Yb-doped core diameter	22 µm	12 µm
Yb doping concentration	$4.5x10^{25}$ m^{-3}	$4.5x10^{25}$ m^{-3}
Core NA	0.048	0.047
Supported core modes	LP_{01}, LP_{11}	LP_{01}, LP_{11}
Doping overlap factor	0.93	0. 54
Doping overlap factor LP_{11}	0.63	0. 15
Effective LP_{01} mode area[b]	281 μm^2	298 μm^2
Cladding pump absorption[a]	1.52 dB/m	0.42 dB/m
Fiber length used for S^2-imaging	2.0 m	2.5 m

[a]Measured at 976 nm.
[b]Calculated at 1060 nm.

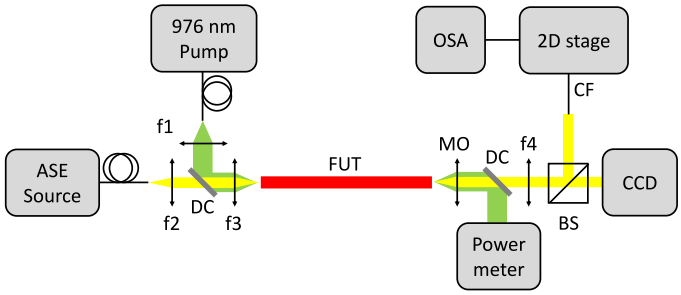

Fig. 4. S^2-measurement setup for mode analysis (DC: Dichroic mirror, FUT: Fiber under test, MO: Microscope objective, BS: Beam splitter).

flexibility in fiber design as it is not restricted to circular symmetric rare-earth-doping profiles such as those manufactured by modified chemical vapor deposition (MCVD). Therefore, it could also be employed to manufacture fibers that provide preferential gain to modes that lack azimuthal symmetry. In this study, we are interested in providing preferential gain to the fundamental Gaussian-like mode and, therefore, we confined the Yb doping to the central 12 μm of the 23 μm diameter core. It has been shown in previous theoretical work that this ratio of core area to doped area is close to the theoretical optimum for HOM suppression [29]. The pump cladding geometry of both fibers has an octagonal shape to guarantee uniform pump distribution; the measured absorption data for both fibers are given in Table I. Based on the measured 2D refractive index data, finite difference simulations have been performed to calculate the profiles of guided core modes (Figs. 3(e) and 3(f)) as well as the spatial overlap of the guided modes with the respective Yb-doped core regions and the effective mode areas (Table I). It is found that both fibers support LP_{01} and LP_{11} modes, however, the overlap factors of the respective modes with the doped regions are significantly different. Therefore, we expect the differential gain between the LP_{01} mode and the LP_{11} mode to be significantly higher in the case of Fiber 2.

IV. Mode Analysis and Pointing Stability

To measure the HOM content of the signal exiting the fiber under test (FUT) as a function of absorbed pump power, the S^2-setup illustrated in Fig. 4 is used. A broadband seed signal is provided by a single mode fiber coupled super luminescence diode (SLD) amplified to ~100 mW average power and with a center wavelength of 1060 nm. A two-lens-telescope (f2 and f3) is used to match the mode field diameter (MFD) of the seed signal to the MFD of the LP_{01} mode of the FUT. Another two-lens-telescope (f1 and f3) and a dichroic mirror (DC) are used to launch 976 nm light from a multimode fiber coupled diode laser into the cladding of the FUT. On the other side of the FUT, a 40x-microscope objective (MO) with 0.48 NA and a lens (f4) with 175 mm focal length are used to image the fiber facet onto a CCD camera (CCD). Another DC is used to separate the 976 nm pump light from the signal. A 90/10 beam splitter cube (BS) directs 90% of the signal power towards a collection fiber (CF) and 10% of the power towards the CCD camera, located at or close to the imaging plane of the 4f imaging system. The CF is mounted on a motorized 2D translation stage and is connected to an optical spectrum analyzer (OSA) to measure signal spectra at different spatial positions across the fiber output facet image. It is highly multimode with a 50 μm core diameter and 0.22 NA and therefore its transfer function can be assumed to be sufficiently flat to resolve multi-mode interference fringes generated in the FUT. A power meter is used measure the transmitted 976 nm pump power. The S^2 measurement is performed by scanning the collection fiber in 50 μm steps across the image of the FUT facet and by recording output spectra at about 400 positions. The modes present in the beam are identified and their power contribution is quantified from the measured spectra following

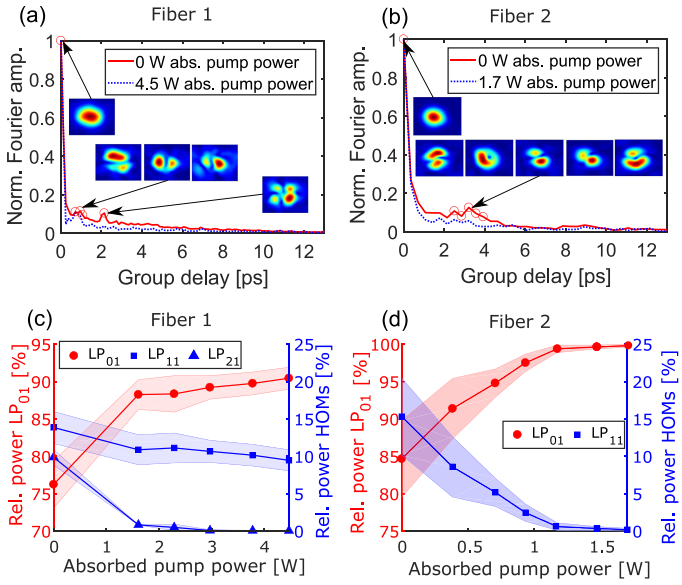

Fig. 5. S^2 measurement results of Fiber 1 and Fiber 2 in an amplifier configuration. (a), (b) Fourier amplitude spectra and reconstructed near field mode profiles. (c), (d) Relative mode power as a function of absorbed 976 nm light.

the standard Fourier-analysis presented in Refs. [26], [30]. The S^2 measurements presented here are measured in the wavelength range between 1020 nm and 1050 nm for Fiber 1 and between 1030 nm and 1040 nm for Fiber 2, respectively, in order to provide sufficient resolution in the time domain. The FUT is kept straight in order to exclude bend induced HOM losses from our considerations. HOM excitation is achieved by intentionally misaligning the FUT from the optical axis of the focused seed beam. During the misalignment procedure, the beam exiting the FUT is monitored with a CCD camera to ensure dominant but not pure fundamental mode excitation. To ensure that the launching conditions didn't change while measuring the HOM content as a function of absorbed pump power, the first S^2-measurement without incident pump light has been repeated at the end of each measurement cycle. The deviation between the two measured HOM contents was less than 0.5 %, which demonstrates the robustness of our set up and method. Figs. 5(a) and 5(b) show four normalized Fourier amplitude spectra of our S^2 measurements for Fiber 1 and Fiber 2 with and without pump light coupled into the FUT. These spectra are the sums of all Fourier transforms measured across the beam cross-section [26], [30]. The peak at 0 ps group delay (GD), often called the DC-peak, corresponds to the power contribution of all the modes present in the beam. The reconstructed near field profiles at a GD of 0 ps is similar to the mode field profile of a LP_{01} mode as we ensured dominant fundamental mode excitation when we coupled the seed signal into the FUT. The other peaks in the Fourier power spectrum arise from intermodal interference in the fiber. As the HOM content is intentionally kept small, it is valid to neglect interference between HOMs [31] and to focus our analysis only on the interference of HOMs with the dominant fundamental mode. To identify which HOMs induce peaks in the Fourier spectrum, near field profiles are reconstructed at the relevant GDs using Fourier filtering as described in Refs. [26], [30] and are provided as insets in Figs. 5(a) and 5(b). For example, the peaks in Fig. 5(a) around a GD of 0.70 ps correspond to the $LP_{11,\,e}$ and $LP_{11,\,o}$ modes that are interfering with the dominant LP_{01} mode. Both LP_{11} modes appear at slightly different GDs in the Fourier spectrum, which indicates the presence of a small anisotropy in Fiber 1 that breaks the degeneracy of the $LP_{11,\,e}$ and $LP_{11,\,o}$ modes. A second peak at a GD of 2.14 ps corresponding to a LP_{21}-like mode interfering with the fundamental mode is also found in the Fourier spectrum of Fiber 1 at low power pump rates (Fig. 5(a)). As the core V-number of ~3.22 indicates, this mode should not be guided by the core of Fiber 1. However, finite difference simulations of the entire fiber structure showed, that due to refractive index variations in the cladding region, LP_{21}-like modes are supported by Fiber 1. The Fourier spectra of Fiber 2, with and without pump light, are shown in Fig. 5(b). In this fiber, a broad peak centered at a GD of ~3.25 ps is observed in the Fourier spectrum. The reconstructed near field images indicate, that the peak corresponds to LP_{11} modes interfering with the fundamental mode.

Next, we investigate the HOM content at the fiber output for both fibers as a function of gain by performing multiple S^2 measurements for different launched pump powers and quantify the HOM content following Refs. [23], [25]. The results of these investigations for Fiber 1 and Fiber 2 are summarized in Figs. 5(c) and 5(d), respectively. Broad maxima in the Fourier domain typically result in less clean mode reconstructions [31]. This causes some uncertainty in obtaining the exact HOM contents of a beam. Here, we illustrate the HOM content as colored symbols indicate the uncertainty through shaded regions in Figs. 5(c) and 5(d). The relative powers carried by the degenerated $LP_{11,\,e}$ and $LP_{11,\,o}$ modes are added together and shown as blue squares in Figs. 5(c) and 5(d). For Fiber 1, the relative power contribution of the LP_{11} modes remains strong across all pump levels. In contrast to the relative content of the LP_{21}-like mode, which decays rapidly with increasing pump, the relative power contribution of the LP_{11} decreases only slightly from ~14% to ~10% as the absorbed pump power increases from 0 W to 4.5 W (see Fig. 5(c)). At the same time, the relative power contribution of the fundamental mode content increases slightly from ~76 % to ~91 % at the highest pump level. This behavior can be explained by the rather large overlap factor of ~63% of the LP_{11} modes with the Yb-doped area in Fiber 1 which has to be compared to a ~93% overlap of the LP_{01} mode and only ~4% overlap of the LP_{21}-like mode.

In striking contrast, a very strong LP_{11} suppression has been observed utilizing our confined doping fiber (Fiber 2) in the amplifier. Already 1.7 W of absorbed pump power is sufficient to reduce the total LP_{11} content from ~15 % to less than ~2% (see Fig. 5(d)). This rigorous HOM suppression at rather low pump levels is a direct consequence of the confined doping design of Fiber 2 and the corresponding strong reduction in overlap of LP_{11} modes with the doped area from ~63% in Fiber 1 to ~15% in Fiber 2.

The degree of HOM suppression in high power fiber amplifiers has important consequences for the pointing stability of the respective beams. The presence of various transverse modes

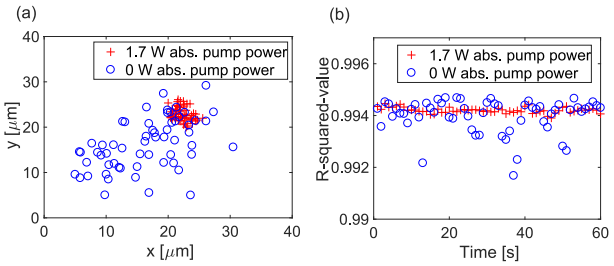

Fig. 6. Beam pointing analysis during perturbation of Fiber 2 with a fan. (a) Beam centroid position on CCD camera. (b) R^2-values of Gaussian 2D fits on beam profile as a function of time.

makes the pointing position extremely sensitive to environmental perturbations of the fiber. Encouraged by our S^2 measurement results, we performed a pointing stability analysis of the Fiber 2 amplifier in the presence of environmental perturbations. Using a fan, we excited small vibrations of a loose segment of Fiber 2 and recorded 60 far field beam profiles using a CCD camera placed 85 cm away from the fiber facet over a time span of one minute. The seed coupling condition was not changed with respect to our previous S^2 measurements and a 5 nm band pass filter centered at 1030 nm was placed in front of the camera. As shown in Figs. 6(a) and 6(b), we performed two pointing stability measurements, one with and one without 976 nm pump light coupled into Fiber 2. The plotted beam centroid positions highlight the drastically improved beam pointing stability due to strong HOM suppression at elevated pump levels in Fiber 2 with confined doping. We also fitted 2D Gaussian distributions to the recorded beam profiles and calculated the R^2-values (Fig. 6(b)), to quantify the beam deformations due to multi-mode interference. While the shape of the beam exiting Fiber 2, in analogy to its centroid position, changes constantly in the absence of pump light, we also observe a strong improvement in beam shape stability as pump light was coupled into Fiber 2 (see Media 1 and Fig. 6(b)), which is another indication for the strong HOM suppression due to gain in Fiber 2.

V. Conclusion

In conclusion, we investigated for the first time the HOM content in beams exiting Yb-doped LMA fibers with and without confined doping as a function of absorbed pump power using S^2 imaging. Our S^2 measurements indicate strong HOM suppression due to differential gain in the case of the confined doping fiber, which is in striking contrast to our findings for the homogenously Ytterbium doped LMA fiber with very limited HOM suppression. We also showed that the HOM suppression drastically improved pointing and shape stability of the beams exiting our confined doping amplifier indicating single mode performance even under imperfect launching conditions and environmental perturbations. Our results, in combination with recent high power experiments using the same fiber [27] and a study that indicated enhanced transverse mode instability (TMI) threshold for a confined doping fiber [32], highlight the potential of confined doping strategies for achieving excellent high power single mode amplifier performance.

References

[1] D. J. Richardson, J. Nilsson, and W. A. Clarkson, "High power fiber lasers: Current status and future perspectives [Invited]," *J. Opt. Soc. Am. B*, vol. 27, no. 11, pp. B63–B92, Nov. 2010.
[2] C. Jauregui, J. Limpert, and A. Tünnermann, "High-power fibre lasers," *Nature Photon.*, vol. 7, pp. 861–867, Oct. 2013.
[3] Y. Baolai *et al.*, "3.05 kW monolithic fiber laser oscillator with simultaneous optimizations of stimulated Raman scattering and transverse mode instability," *J. Opt.*, vol. 20, no. 2, 2018, Art. no. 025802.
[4] K. Shima, S. Ikoma, K. Uchiyama, Y. Takubo, M. Kashiwagi, and D. Tanaka, "5-kW single stage all-fiber Yb-doped single-mode fiber laser for materials processing," in *Proc. SPIE LASE*, 2018, vol. 10512, Art. no. 6.
[5] C. X. Yu, O. Shatrovoy, T. Y. Fan, and T. F. Taunay, "Diode-pumped narrow linewidth multi-kilowatt metalized Yb fiber amplifier," *Opt. Lett.*, vol. 41, no. 22, pp. 5202–5205, Nov. 2016.
[6] F. Beier *et al.*, "Single mode 4.3 kW output power from a diode-pumped Yb-doped fiber amplifier," *Opt. Express*, vol. 25, no. 13, pp. 14892–14899, Jun. 2017.
[7] T. Sosnowski *et al.*, "3C Yb-doped fiber based high energy and power pulsed fiber lasers," in *Proc. SPIE LASE*, 2013, vol. 8601, Art. no. 11.
[8] J. M. Fini, "Design of solid and microstructure fibers for suppression of higher-order modes," *Opt. Express*, vol. 13, no. 9, pp. 3477–3490, May 2005.
[9] C. Pare, P. Laperle, H. Zheng, and A. Croteau, "Multi-cladding fiber," ed: Google Patents, 2014.
[10] Z. Sanjabi Eznaveh, J. E. Antonio-Lopez, J. Anderson, A. Schülzgen, and R. Amezcua-Correa, "Reduced-symmetry LMA rod-type fiber for enhanced higher-order mode delocalization," *Opt. Lett.*, vol. 42, no. 10, pp. 1974–1977, May 2017.
[11] J. P. Koplow, D. A. V. Kliner, and L. Goldberg, "Single-mode operation of a coiled multimode fiber amplifier," *Opt. Lett.*, vol. 25, no. 7, pp. 442–444, Apr. 2000.
[12] J. Limpert *et al.*, "Yb-doped large-pitch fibres: Effective single-mode operation based on higher-order mode delocalisation," *Light: Sci. Amp; Appl.*, vol. 1, p. e8, Apr. 2012.
[13] J. R. Marciante, R. G. Roides, V. V. Shkunov, and D. A. Rockwell, "Near-diffraction-limited operation of step-index large-mode-area fiber lasers via gain filtering," *Opt. Lett.*, vol. 35, no. 11, pp. 1828–1830, Jun. 2010.
[14] D. Jain, Y. Jung, M. Nunez-Velazquez, and J. K. Sahu, "Extending single mode performance of all-solid large-mode-area single trench fiber," *Opt. Express*, vol. 22, no. 25, pp. 31078–31091, Dec. 2014.
[15] L. Huang, L. Kong, J. Leng, P. Zhou, S. Guo, and X. A. Cheng, "Impact of high-order-mode loss on high-power fiber amplifiers," *J. Opt. Soc. Am. B*, vol. 33, no. 6, pp. 1030–1037, Jun. 2016.
[16] R. T. Schermer and J. H. Cole, "Improved bend loss formula verified for optical fiber by simulation and experiment," *IEEE J. Quantum Electron.*, vol. 43, no. 10, pp. 899–909, Oct. 2007.
[17] C. Schulze *et al.*, "Mode resolved bend loss in few-mode optical fibers," *Opt. Express*, vol. 21, no. 3, pp. 3170–3181, Feb. 2013.
[18] P. Stremplewski and C. Koepke, "ASE noise independent small signal modal gain measurements and mode imaging in double clad Nd^3+- doped fiber around 900 nm," *Opt. Express*, vol. 22, no. 20, pp. 24847–24858, Oct. 2014.
[19] S. Wittek *et al.*, "Mode-selective amplification in a large mode area Yb-doped fiber using a photonic lantern," *Opt. Lett.*, vol. 41, no. 10, pp. 2157–2160, May 2016.
[20] J. M. Sousa and O. G. Okhotnikov, "Multimode Er-doped fiber for single-transverse-mode amplification," *Appl. Phys. Lett.*, vol. 74, no. 11, pp. 1528–1530, 1999.
[21] C. Seah, W. Lim, and S.-L. Chua, "A 4kW fiber amplifier with good beam quality employing confined-doped gain fiber," in *Proc. Adv. Solid State Lasers*, 2018, p. AM2A. 2.
[22] L. Liao *et al.*, "Confined-doped fiber for effective mode control fabricated by MCVD process," *Appl. Opt.*, vol. 57, no. 12, pp. 3244–3249, Apr. 2018.
[23] C. Ye, J. Koponen, T. Kokki, J. M. I. Ponsoda, A. Tervonen, and S. Honkanen, "Confined-doped ytterbium fibers for beam quality improvement: Fabrication and performance," in *Proc. SPIE LASE*, 2012, vol. 8237, Art. no. 7.
[24] T. Kokki, J. Koponen, M. Laurila, and C. Ye, "Fiber amplifier utilizing an Yb-doped large-mode-area fiber with confined doping and tailored refractive index profile," in *Proc. SPIE LASE*, 2010, vol. 7580, Art. no. 9.
[25] V. Roy, C. Paré, P. Laperle, L. Desbiens, and Y. Taillon, "Yb-doped large mode area fibers with depressed clad and dopant confinement," in *Proc. SPIE LASE*, 2016, vol. 9728, Art. no. 7.

[26] J. W. Nicholson, A. D. Yablon, S. Ramachandran, and S. Ghalmi, "Spatially and spectrally resolved imaging of modal content in large-mode-area fibers," *Opt. Express*, vol. 16, no. 10, pp. 7233–7243, May 2008.
[27] A. S. Justin Cook, J. E. Antonio-Lopez, S. Gausmann, A. Schülzgen, R. A. Correa, and M. Richardson, "Diagnostics and design parameters for kW-class Yb fiber lasers," presented at the SPIE Photon. West, San Francisco, 2019.
[28] A. V. Smith and J. J. Smith, "Mode competition in high power fiber amplifiers," *Opt. Express*, vol. 19, no. 12, pp. 11318–11329, Jun. 2011.
[29] J. R. Marciante, "Gain filtering for single-spatial-mode operation of large-mode-area fiber amplifiers," *IEEE J. Sel. Topics Quantum Electron.*, vol. 15, no. 1, pp. 30–36, Jan. 2009.
[30] J. W. Nicholson, A. D. Yablon, J. M. Fini, and M. D. Mermelstein, "Measuring the modal content of large-mode-area fibers," *IEEE J. Sel. Topics Quantum Electron.*, vol. 15, no. 1, pp. 61–70, Jan. 2009.
[31] C. Jollivet, D. Flamm, M. Duparré, and A. Schülzgen, "Detailed characterization of optical fibers by combining S^2 imaging with correlation filter mode analysis," *J. Lightw. Technol.*, vol. 32, no. 6, pp. 1068–1074, Mar. 2014.
[32] F. Zhang *et al.*, "Gain-tailored Yb/Ce codoped aluminosilicate fiber for laser stability improvement at high output power," *Opt. Express*, vol. 27, no. 15, pp. 20824–20836, Jul. 2019.

Stefan Gausmann, received the B.S. and M.S. degrees in physics from RWTH Aachen University, Aachen, Germany, in 2014 and 2016, respectively, and the M.S. degree in optics and photonics, in 2017, from the University of Central Florida, Orlando, FL, USA, where he is currently working toward the Ph.D. degree. His current research interests include CW and pulsed kW fiber lasers as well as optical fiber characterization.

Jose E. Antonio-Lopez, biography not available at the time of publication.

James Anderson, biography not available at the time of publication.

Steffen Wittek received the M.Sc. degree in optics and photonics from CREOL, The College of Optics and Photonics, University of Central Florida, Orlando, FL, USA, where he is currently working toward the Ph.D. degree. His current research interests include optical fiber devices, high-power fiber amplifiers, and spatial multiplexing. He has authored more than 14 scientific publications in peer-reviewed journals and conference proceedings.

Sanjabi Eznaveh Eznaveh, biography not available at the time of publication.

Hee-Jun Jang, biography not available at the time of publication.

Md Selim Habib, biography not available at the time of publication.

Justin Cook received the B.S. degrees in physics and applied mathematics from Austin Peay State University, Clarksville, TN, USA, in 2015 and the M.S. degree in optics from CREOL, College of Optics and Photonics, University of Central Florida, Orlando, FL, USA, in 2015, where he is currently working toward the Ph.D. degree in the optics program. As a Graduate Research Assistant with the Laser Plasma Laboratory, his primary research interests include designing and constructing high-power and high-energy fiber lasers. Additional research interests include mid-infrared materials and sources, nonlinear effects in optical fibers, and laser materials processing.

Martin C. Richardson, biography not available at the time of publication.

Rodrigo Amezcua Correa, biography not available at the time of publication.

Axel Schlzgen received the Ph.D. degree in physics from the Humboldt University of Berlin, Berlin, Germany, in 1992. Since 2009, he has been a Professor of Optics and Photonics, CREOL, The College of Optics and Photonics, University of Central Florida, Orlando, FL, USA. He also holds an Adjunct Research Professor position with the College of Optical Sciences, University of Arizona. His current research interests include optical fiber devices, components, materials, and structures with applications in fiber laser systems, fiber optic sensing and imaging, and optical communications. He has authored more than 130 scientific publications in peer-reviewed journals, more than 60 invited talks at international conferences, and six patents. He is a Fellow of the Optical Society of America.